INVESTIGATIONS OF SURFACE ROUGHNESS LENGTH MODIFICATION IN BLACK ROCK CITY, NV

A Thesis submitted to the faculty of
San Francisco State University
In partial fulfillment of
the requirements for
the Degree

Master of Science
In
Geographic Information Science

by

Garrett Ross Bradford

San Francisco, California

January 2015

CERTIFICATION OF APPROVAL

I certify that I have read Investigations of Surface Roughness Length Modification in Black Rock City, NV by Garrett Ross Bradford, and that in my opinion this work meets the criteria for approving a thesis submitted in partial fulfillment of the requirement for the degree Master of Science in Geographic Information Science at San Francisco State University.

Andrew Oliphant, Ph.D.
Professor of Geography

Leonhard Blesius, Ph.D.
Associate Professor of Geography

INVESTIGATIONS OF SURFACE ROUGHNESS LENGTH MODIFICATION IN BLACK ROCK CITY, NV

Garrett Ross Bradford
San Francisco, California
2015

The objective of this study is to investigate changes to the surface roughness length (z_0) and zero-plane displacement height (z_d) in Black Rock City, Nevada (BRC) during the Burning Man festival in 2013. The surface parameters are estimated using both anemometric and morphometric methods. Estimated z_0 values were much larger than a typical playa surface but remained smaller than a typical urban or suburban area. Anemometric methods result in large scatter, but generate reasonable results. Removal of slightly-unstable periods lowers scatter and improves reasonableness of observational estimates of z_d. Morphometric estimates predict an early peak in z_0 and an increase in z_d throughout the event. Based on these results, this morphometric approach appears valid for use in BRC or other temporary cities.

I certify that the Abstract is a correct representation of the content of this thesis.

_____ _____

Chair, Thesis Committee Date

ACKNOWLEGEMENT

This work would not have been possible without a large number of people. I will attempt to list them here and hope that I get them all. Maureen Bradford, Andrew Oliphant, Leonhard Blesius, Malori Redman, Ryan Thorp, Craig Clements, Doris (Swampy) Dialogu, Lewis Ames, Damien Reggio, Michal Minecki, Todd Huffman, all the members of Camp A.N.T.E.N.A., and all the citizens of Black Rock City.

TABLE OF CONTENTS

LIST OF TABLES

Table Page

LIST OF FIGURES

Figure Page

1 Introduction

Estimates of surface roughness length (z_0) and zero-plane displacement height (z_d) are vital to the study of urban microclimates. These parameters are necessary for examining the behavior of turbulence in urban areas, engineering applications involved with local wind structure, modeling air pollution, and representing the impact of urban areas on weather and climate in numerical models (Al-Jiboori & Fei, 2005; Liu *et al*., 2009). While simple rule-of-thumb or land-use/land-cover (LULC) look-up tables can be used as model inputs, these values may differ substantially from actual surface morphometry. Additionally, heterogeneous arrays of roughness elements within urban areas may cause z_d and z_0 to vary, not only spatially but also directionally with wind. To better characterize the nature of these surface parameters in urban environments, recent studies have relied on a wide range of anemometric and morphometric techniques (Grimmond *et al*., 1998; Grimmond & Oke, 1999; Al-Jiboori & Fei, 2005; Liu *et al*., 2009; Di Sabatino, *et al*., 2010).

The objective of this study is to investigate changes to the surface parameters z_0 and z_d in Black Rock City, Nevada (BRC) during the Burning Man festival in 2013. While it differs dramatically from most modern cities, BRC has many characteristics associated with local scale climate modification in urban areas, particularly the role of physical structures on turbulence and the surface layer wind profile. Unlike previous studies, data from BRC allows for the evaluation of roughness parameters over a range of object densities because the city developed rapidly over the period of a week around the

experiment site. This paper presents the results of the investigation from both fast-response anemometry and an analysis of surface morphometry. A brief introduction into the role of z_0 in the lower level wind profile is followed by a description of the study site, the experiment design, and the methods used. The results of the study are then presented and compared.

2 Surface Roughness and the Boundary Layer Wind Profile

The planetary boundary layer (PBL) below the inversion height (z_i) is composed of three different sub-layers. The lowest of these is the roughness sub-layer (RSL), above which is the inertial sub-layer (ISL), followed by the mixed layer (ML) (Figure 1). The RSL and ISL together comprise the surface layer (SL), where atmospheric conditions are influenced by the upwind surface characteristics. Because of the height and density of structures in urban areas, the vertical exchanges of momentum generally do not occur at the surface and instead occur within the urban canopy layer (UCL). Within this layer, atmospheric conditions are driven by local surface types and obstacles, and not generally representative of the area as a whole. Height of the UCL is about that of the average roughness obstacle height (z_H) and while the RSL may range from $1.5z_H$ in dense areas to $4z_H$ in low-density areas (Oke 2006).

Within the SL, the wind field is affected by frictional drag imposed by the underlying rigid surface. As wind passes over a surface, the air exerts a shearing stress on that surface. This is equal to the force exerted by the surface on the PBL. The surface layer of frictional influence generates a shearing force and transmits it downwards as a flux of momentum. The mean horizontal momentum possessed by different levels is proportional to the profile of wind speed, which increases logarithmically with height (z). Under conditions of neutral stability, mean wind speed ($\bar{u}$) at height z can be described by Monin-Obukov (M-O) wind profile:

$$\bar{u}_z = \frac{u_*}{k} \ln\left(\frac{z'}{z_0}\right)$$

Equation 1

where u_* is the friction velocity, k is von Karman's constant (~0.4), and $z' = z - z_d$.

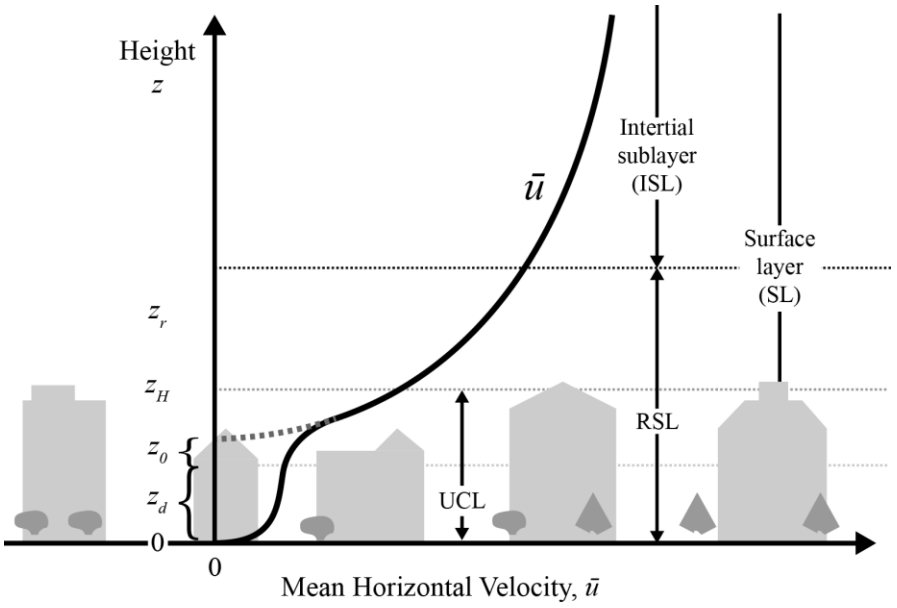

Figure 1: Generalized mean wind velocity in a densely developed urban area showing the location of the sub-layers of the surface layer. The height scale shows the height of the roughness sub-layer (z_r), the mean height of roughness elements (z_H), the roughness length (z_0), and the zero-plane displacement height (z_d). The dotted grey line is the profile extrapolated from the inertial sub-layer and the solid line the actual profile. Modified after Oke (2006).

In theory, z_0 is the height where the neutral wind profile reaches zero (dashed line in Figure 1). z_0 is related to the height, shape, density, and spacing of roughness elements in the upwind area. Over complex terrain, such as urbanized areas, the compactness of

roughness elements can create a skimming effect such that z_0 is raised to some level above the ground. This skimming flow may raise the level of the mean momentum sink creating a new surface datum at z_d (Liu *et al.*, 2009). Failure to incorporate z_d in urban areas may lead to a gross overestimation of surface roughness (Grimmond & Oke, 1998). Equation 1 assumes a thermally neutral surface layer as well as a homogenous source area. When these conditions are not met, $z_0, z_d,$ and u_* are simply curve fitting parameters and may lack physical meaning (Bottema, 1997).

Table 1: Roughness Lengths (z_0) for Homogenous Surface Types

Surface Type	Roughness length (m)	
	min	max
Sea, loose sand and snow	0.0002	0.0002
Concrete, flat desert, tidal flat	0.0002	0.0005
Flat snow field	0.0001	0.0007
Rough Ice Field	0.001	0.012
Fallow ground	0.001	0.004
Short grass and moss	0.008	0.03
Long grass and heather	0.02	0.06
Low mature agricultural crops	0.04	0.09
High mature crops ("grain")	0.12	0.18
Continuous bushland	0.35	0.45
Mature pine forest	0.8	1.6
Tropical forest	1.7	2.3
Dense low buildings ("suburb")	0.4	0.7
Regularly-built large town	0.7	1.5

Source: Wieringa (1993)

Typical roughness lengths are shown in Table 1. These values are based on field studies and are often used in combination with land-use/land-cover data to estimate effective roughness values (Powell, 2005; Wieringa, 1993). While suburban and urban

areas represent some of the roughest surfaces on the planet, the nature of z_d and z_0 is relatively poorly understood for these areas. In part, this is because of the difficulty in observational methods in urban areas due to expense and site selection (Oke, 2006; Grimmond *et al*., 1998). Additionally, the heterogeneity within and between urban sites makes classification and modeling of these areas harder as compared to more homogenous landscapes.

3 Description of Site and Experiment

The experiment was conducted over an eleven-day period in 2013 (DOY 234 - 245) in the Black Rock Desert, Nevada (BRD; 119°12'24" W 40° 47'5" N; 1,190 m a.s.l.), during the Burning Man festival. BRD is the site of an extensive playa surface characterized by flat, homogenous terrain devoid of vegetation. Playa surfaces of this type are generally classified as extremely smooth ($z_0 \sim 0.05$ cm; Wieringa, 1993). The smooth playa surface provides a useful reference for this study because any observed change to the surface roughness length may be attributable to the addition of human structures. Once a year, a portion of the playa is transformed into a temporary metropolis known as Black Rock City (BRC). In 2013, the peak recorded population of BRC was 69,613 (Afterburn Report 2013). The properties of the normally flat, homogeneous surface are quickly altered by the addition of vehicles, shipping containers, tents, and structures of a variety of shapes and sizes. In contrast to the bare playa surface, where roughness features are on the order of 0.01 m, the roughness elements of BRC are on the order of 1-10 m.

The experimental set up consisted of instruments deployed on a 32 m telescoping, steel-lattice tower (Clements & Oliphant, 2014). The tower was situated within a densely populated neighborhood such that the fetch in the predominate wind direction was entirely "urban" (See Figures 2 and 3). Instruments were oriented into the predominate wind direction, with booms extending east-west from the tower to avoid wake effects. Temperature, relative humidity, horizontal wind speed and direction were measured at six

heights: z_1=27.5 m; z_2=19.7 m; z_3=11.6 m; z_4=8 m, z_5=5 m, and z_6=3 m. Additionally, z_3 was equipped with a fast-response, three-dimensional sonic anemometer for eddy covariance and turbulence measurements. The tower was deployed four days prior to the start of the Burning Man event to collect base-line measurements before the major development of the city. However, due to permitting constraints, no observations were made over completely undeveloped playa. Initial data processing for this analysis consisted of calculating 30-min averages for each observation period where reliable data was available.

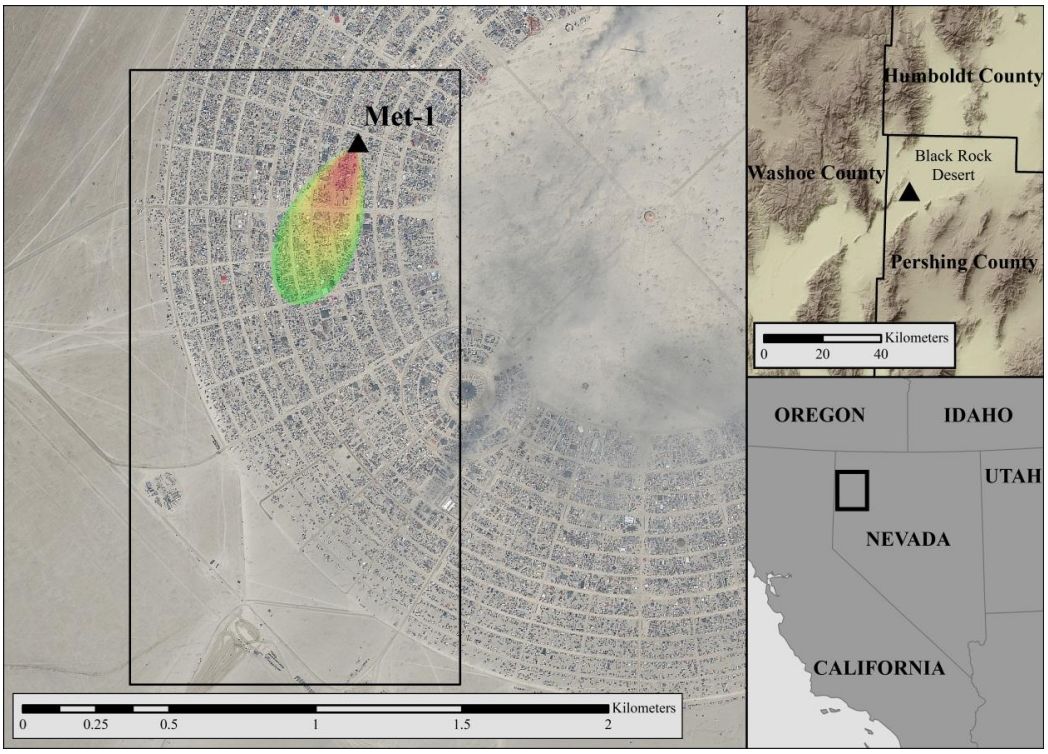

Figure 2: On the left, World-View 2 satellite image of Black Rock City (BRC) showing the location of the tower. Color shaded area shows the extent of the source area contributing 75% of the flux concentration at 11.7 m using the method of Hsieh *et al.* (2000). Black rectangle in left-hand map shows area of analysis for morphometric methods. On the right, overview maps showing the location of BRC (top) and Black Rock Desert (bottom).

Figure 3: Oblique, south-facing view at 27.5 m. The left hand image was captured on DOY 234 and the right on 242.

4 Methods

Methodology for estimating surface roughness can be divided into two broad categories: anemometric and morphometric. The former uses field observations of wind or turbulence and is based on theoretical relations derived from the logarithmic wind profile (Equation 1). The earliest methods of this type use profiles of wind observations to estimate u_* and z_0 whereas more recent methods use direct observations of turbulence to calculate u_* (Grimmond *et al.*, 1998). Morphometric algorithms relate aerodynamic parameters to measures of surface morphometry. The simplest methods of this type are rule-of-thumb approaches that estimate z_d and z_0 as a percentage of average obstacle or canopy height while more sophisticated algorithms incorporate obstacle size, spacing, and the frontal area projected into the on-coming wind direction (Grimmond & Oke, 1999).

Morphometric methods are advantageous in that they can be obtained for any wind direction and without the need for towers and instrumentation. Their results, however, are based on empirical relations derived from wind tunnel work, which can differ substantially from reality when objects are irregularly spaced and wind direction is constantly changing (Grimmond & Oke, 1999). Anemometric methods do not require any surface type specification; however, they are expensive, difficult to obtain, and can only be applied during specific atmospheric conditions. This study relies on a combination of both types of methods to characterize modification to the roughness parameters over BRC and to allow for a comparison of their results.

4.1 Anemometric

In their review of anemometric methods, Grimmond *et al.* (1998) used only one observational method to estimate z_d (temperature variance method, Tv). In their analysis, Tv did not produce reasonable results for three out of the four sites studied. These authors questioned whether the central assumptions of this method – that source areas are thermally homogenous and that the sources/sinks of temperature and momentum are co-located – were valid for urban areas in general. Rooney (2001) reported the same result from the Tv method and instead relied on the M-O profile to estimate z_d. Perhaps because of the lack of reliable methods, most studies of z_0 using anemometric methods in urban areas use morphometric methods to estimate z_d.

The present study uses the Rooney displacement method (Ro) to estimate z_d during the course of the Burning Man event. Ro uses measurements of friction velocity and wind speed from two heights to calculate z_d for each observation period:

$$z_{d\,Ro} = \frac{z_1 e^{-ku_1/u_*} - z_2 e^{-ku_2/u_*}}{e^{-ku_1/u_*} - e^{-ku_2/u_*}}$$

Equation 2

Following the criteria of Rooney (2001), the available data was limited to periods of near-neutral stability and then binned into 45° sectors. Near-neutral stability was defined by the dimensionless stability parameter ($\zeta = z'/L$, where L is the Obukov length), such that $|\zeta| < 0.1$. Additionally, a minimum of ten observation periods is recommended to calculate an average value due to the potential for large scatter in the resulting estimates.

Unlike Rooney (2001), only one three-dimensional sonic anemometer was available for this study so the stability filtering was only applied to data from one level (z_3). While u_* is assumed to be constant with height in Equation 1, Rooney (2001) employed an additional check on this assumption that was not available here. Data from z_3 and z_5 were used to calculate z_d for each directional sector. Additionally outliers were removed by filtering out periods where any of the observation levels differed significantly from the M-O profile by ensuring that $\bar{u}_1 > \bar{u}_2 > \bar{u}_3 > \bar{u}_4 > \bar{u}_5 > \bar{u}_6$, where $\bar{u}_i$ is the mean wind speed at height z_i.

Unlike z_d, there is a larger body of literature on estimating z_0 from wind observations (Grimmond *et al.*, 1998). While anemometric methods are considered the standard, there is no 'best' method to estimate this parameter. Observational methods are divided into slow- and fast-response techniques. The former rely on a profile of mean wind speed observations or standard deviation at a single level. With the use of fast-response, three-dimensional sonic anemometry it is possible to calculate u_* directly and z_0 can then be determined from Equation 1, provided z_d is known (the eddy covariance stress method henceforth called Es).

In previous studies, slow-response methods tended to perform poorly with respect to both fast-response and morphometric approaches (Al-Jiboori & Fei, 2005; Grimmond *et al.*, 1998). Because of this and the availability of fast-response observations, the Es method was used here. The same filtering of observation periods used for z_d were applied to this method. Al-Jiboori & Fei (2005) recommend a minimum of twenty observations

($N \geq 20$) per directional sector for estimates to be valid. Grimmond *et al*. (1998) also noted this minimum requirement; however, it was relaxed to five observations ($N \geq 5$) in that study because of the scarcity of data points available for analysis. Additionally, observation periods where wind speed was less than 2 m s^{-1} were excluded. This is higher than the 1 m s^{-1} recommended in Liu (2009); however, preliminary results indicated that periods with mean wind speed < 2 m s^{-1} tended toward unrealistically large estimates and were removed.

4.2 Morphometric

Similar to anemometric methods, there is no one 'best' morphometric model. In their review, Grimmond & Oke (1999) divide these models into three categories: "rule of thumb" height-based approaches, those based on plan area aspect ratios, and those based on frontal area aspect ratios. This analysis uses the third type following the equations developed by MacDonald *et al.*, 1998 (Ma). The Ma model was chosen because it was designed to work in areas of high roughness object densities, the relative ease of implementation, and because it has been widely used to estimate roughness in urban areas (MacDonald *et al.*, 1998; Grimmond & Oke, 1999; Di Sabatino *et al.*, 2010).

Ma is derived from the log-wind profile and relies on three measures of surface morphometry: average obstacle height (z_H), plan area index (λ_p), and frontal area index (λ_f). z_d is calculated using λ_p which is the ratio of the plan area of obstacles (A_p) to total lot area (A_T) whereas z_0 is calculated using λ_f which is the ratio of the frontal area of obstacles (A_f) to A_T (Figure 4):

$$\frac{z_d}{z_H} = 1 + \alpha^{-\lambda_P}(\lambda_P - 1)$$

Equation 3

$$\frac{z_0}{z_H} = \left(1 - \frac{z_d}{z_H}\right) exp\left\{-\left[0.5\beta\frac{C_D}{k^2}(1 - \frac{z_d}{z_H})\lambda_F\right]^{-0.5}\right\}$$

Equation 4

where C_D is the drag coefficient (1.2), α is an empirical coefficient, and β is a correction factor for the drag coefficient. MacDonald *et al.* (1998) recommend $\alpha = 4.43$ and

$\beta = 1.0$ for staggered arrays of cubes. Because the built environment of BRC was irregular rather than uniform, these values were used here.

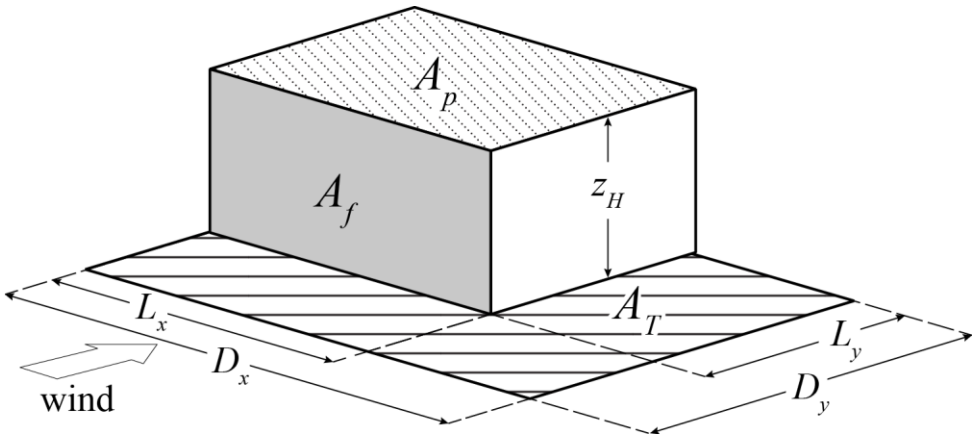

Figure 4: Definition of surface obstacle dimensions used in morphometric analysis. Using these measurements, the non-dimensional ratios are defined as $\overline{\lambda_p} = \overline{A_p}/\overline{A_T}$ and $\overline{\lambda_f} = \overline{A_f}/\overline{A_T}$ where the over-bar denotes the average across all obstacles in a neighborhood area, λ_p is the plan area index, λ_f the frontal area index, A_p the plan area of the obstacle, A_f the frontal area, and A_T the total lot area. Modified after Grimmond & Oke (1999).

To derive the input surface parameters, λ_f and λ_p, a roughness object database was created. The horizontal extent of each obstacle is based on a satellite image of BRC taken on August 29, 2013 (DOY 241) at 19:20 UTC (11:20 local time) when the city was fully populated. The scene was captured by WorldView-2 and has 0.5 m panchromatic resolution and 2.0 m multispectral resolution. The multispectral image was pansharpened to 0.5 m using a hyperspherical color space (HCS) resolution merge method and the resulting image clipped to the bounding box shown in Figure 2 using ERDAS Imagine.

The subset was created to both ease classification and increase image processing speed. The area was selected to restrict the analysis to the sectors that fell within the predominate wind direction as only these provide valid comparisons to the anemometric estimates.

Based on an image segmentation and object-oriented classification in eCognition the image was divided into two classes: "playa" and "other." A simple binary classification was used because of the large variety of object types. Additionally, because of the temporary nature of the city and the speed of its development, complete field surveys for the necessary ground-truthing of a more complex classification were infeasible. Limited field surveys combined with additional aerial and ground photographs were used to check the positional accuracy of the image and for validation of the final classification. The classification rule set was entirely supervised and additional manual corrections were made to ensure that large open areas with disturbed playa sediment were not classified as "other." Other manual changes included the removal of any vehicles in the streets and the deletion of any objects classified as "other" with an area less than 5 m^2 to remove erroneous obstacles created by bicycles or pedestrians.

An additional simplifying assumption was needed to assign z_H because of the binary classification system. While some obstacles were taller than 10 m, the majority of objects surveyed ranged from 1.5 – 4 m with small tents and passenger cars on the low end and RVs, trucks, and shipping containers on the high end of this range. Based on this range, 2.5 m was selected for the average obstacle height. Because of the uncertainty

involved in any method of roughness estimation and this study's focus on the rate of change in z_0 and z_d rather than their absolute values, this assumption seems reasonable.

For morphometric methods a "local" scale approach (10^2-10^3 m) is appropriate in order to assess the effective impact of all roughness obstacles rather than their individual, micro-level effects (Grimmond & Souch, 1994). However, the appropriate neighborhood size for calculating the input parameters λ_f and λ_p is unclear. On the one hand, morphometric analyses should avoid over-emphasizing individual roughness elements. On the other, too large of an area may average out real differences in surface form. For urban areas, Millward-Hopkins *et al*. (2011a) cite a range of resolutions from recent literature of 150 m – 1 km. While BRC represents a dense urban area, the horizontal extent of obstacles is significantly smaller than a typical North American city where the majority of morphometric models are applied. All city blocks in BRC were 60 m deep and varied in length between 150 – 300 m. In contrast with a typical North American home of 200 m^2, the majority of obstacles in BRC are less than 100 m^2 (Figure 5). For this study, λ_f and λ_p were calculated for 25, 50, 100, 150, and 200 m grids to assess the effect of grid size on the results.

To estimate the changes to z_0 and z_d throughout the course of the city's development, the final object database was sampled down proportionally based on estimated total city population using arrival statistics provided by the Black Rock Census. The database of roughness objects was imported into ArcGIS from eCognition and a random selection process was scripted to create a representative obstacle database for each day prior to

DOY 241. λ_f and λ_p were then calculated and used to assess z_0 and z_d by neighborhood grid cell for each day leading up to the capture of the satellite image.

To estimate the effective roughness parameters at the tower location and to compare the morphometric estimates to anemometric results, the footprint model of Hsieh *et al.* (2000) was used to weight the output z_0 and z_d following the method of Grimmond & Oke (1999). The Hsieh footprint model (H_{fp}) is one-dimensional in the original format, meaning the source weight is only expressed along the mean wind direction. Following Joy (2011), a crosswind diffusion function was added to the original model to allow for a two-dimensional source weight function. H_{fp} was selected because of the availability of code and because this relatively simple model has been shown to produce similar results to more complex models (Hsieh, *et al.*, 2000; Joy 2011). The model was implemented in MATLAB for a 5 m grid rotated into the mean wind direction and then exported to ESRI ASCII GRID format (see Figure 3 for illustration). The resulting surface was then used to weight modeled z_0 and z_d from the above listed neighborhood grids according to Equation 5:

$$(\ln z_0^{eff}) = \sum_{i=1}^{n} \left[(\ln z_{0_i}) w_i \right]$$

Equation 5

where w_i is the weight assigned to a given 5 x 5 m cell and z_0^{eff} is the final effective surface roughness value for a directional sector.

Figure 5: Aerial photo of Black Rock City 2013 georeferenced to satellite image. Photo credit: Todd Huffman.

5 Results and Discussion

5.1 Anemometric

There was a clear difference in the surface characteristics prior to the gates opening and during the event itself (Figure 3). In the former period, there were structures and automobiles on the playa surface, however, these were scattered and infrequent. Once the gates opened the number and density obstacles spiked overnight. Based on this visual inspection and arrival statistics, data was separated into two periods for analysis: Pre-Event and Event Week. The former represents all observation periods prior to DOY 238 when the gates opened for general admission and the latter all measurements from DOY 238-245.

Table 2: Number of Observation Periods (*N*) by Direction Sector

Sector	Direction (°)	All Conditions			Near-Neutral Periods		
		Total	Pre-Event	Event	Total	Pre-Event	Event
I	0-45	13	3	10	1	0	1
II	45-90	40	4	36	3	1	2
III	90-135	28	4	24	1	0	1
IV	135-180	75	24	51	14	5	9
V	180-225	284	106	178	144	55	89
VI	225-270	64	25	39	35	17	18
VII	270-315	14	5	9	3	0	3
VIII	315-360	6	1	5	1	0	1

The number of observations (*N*) by 45° sector during each period is shown in Table 2 for both all stability and near-neutral conditions. While the dimensionless stability parameter (ζ) relies on z_d, a sensitivity analysis for a range of possible z_d values for BRC (0 – 2 m) did not significantly change the number of observation periods filtered for

analysis, so $z' = z$ was assumed for filtering observation periods. Because of a strong predominate wind direction only sectors V and VI met the minimum number of observations recommended for the Ro method and only sector V met the minimum number for the Es method (Table 2). However, analysis will be shown for all Sectors with $N \geq 5$.

Table 3: Estimated z_d (m) Statistics by Directional Sector Using the Ro Method

Sector	Direction (°)	Pre-Event (DOY 234-237)				Event (DOY 238-245)			
		N	Median	Mean	SD	N	Median	Mean	SD
IV	135-180	5	0.42	0.71	2.27	6	1.04	0.81	0.97
V	180-225	53	-1.23	-1.76	3.03	88	1.01	0.30	2.02
VI	225-270	11	0.66	0.25	2.52	17	-0.39	-0.44	1.38

The results of the Ro method to estimate z_d are presented in Table 3. The standard deviation (SD) of estimated z_d values exceeded the mean and median z_d values in all cases except Sector IV during the Event Week. Additionally, the Ro method estimated a negative mean z_d in the case of Sector V Pre-Event and Sector VI Event Week, which is theoretically impossible. While the large variability and negative values raise questions about the Ro method's validity, the results appear to indicate an increase in z_d values in Sector V between Pre-Event and Event Week observations (Table 3). In other words, as the city developed after DOY 238, the density of roughness elements was sufficient to raise the effective momentum sink above the surface level within Sector V. In Sector IV the same effect is evident and the values for both Pre-Event and Event Week appear reasonable, however, the number of observation periods is well below the recommended value. This increase in z_d is not apparent in Sector VI; however, it is unclear if this is due

to the smaller sample size or actual differences in surface morphometry relative to Sector V.

Table 4: Estimated z_0 (m) Statistics by Directional Sector Using the Es Method

Sector	Direction (°)	Pre-Event (DOY 234-237)				Event (DOY 238-245)			
		N	Median	Mean	SD	N	Median	Mean	SD
IV	135-180	5	0.09	0.07	0.04	6	0.05	0.10	0.12
V	180-225	53	0.12	0.15	0.11	88	0.16	0.20	0.13
VI	225-270	11	0.25	0.34	0.24	17	0.34	0.33	0.10

The results of the Es method for estimating z_0 are presented in Table 4. For Pre-Event estimates, $z_d = 0$ was assumed whereas for Event Week estimates, the median z_d value from Sector V (1.01 m) was used in calculating z_0. While the uncertainty of this estimate is large, $z_d \sim 1.0\ m$ was appropriate given the rule-of-thumb that z_d is approximately two-thirds the average structure height (Grimmond & Oke, 1998) and that unlike other urban areas, many of the roughness elements in BRC are extremely porous and may not produce the same skimming effect as buildings that completely block air flow. Additionally, due to the relatively small z_d values estimated for this site, the Es method is not as sensitive to z_d as it would be in typical urban areas where this value may reach five to ten times this height. When $z_d = 0$ is assumed, the resulting z_0 values only increase by about 0.01 m.

Similar to the results of the Ro method, the variability in the estimated mean z_0 value was relatively large for all sectors. Both the mean and median values in Sectors V increased slightly between the two periods indicating an increase in z_0 with the development of the city. However, this increase is relatively small given the large

variability and the dramatic change in surface morphometry. Despite a largely undeveloped fetch during the Pre-Event period, the estimated mean z_0 is substantially larger than expected for a bare playa surface (Table 1). In Sector VI the median increased while the mean remained unchanged during Event Week. Both the estimated mean and median z_0 for Sector VI are roughly twice that of Sector V. The SD in the Pre-Event estimates for Sector VI is substantially larger than the Event Week estimates. This larger scatter may be partially a result of the rapidly changing surface conditions.

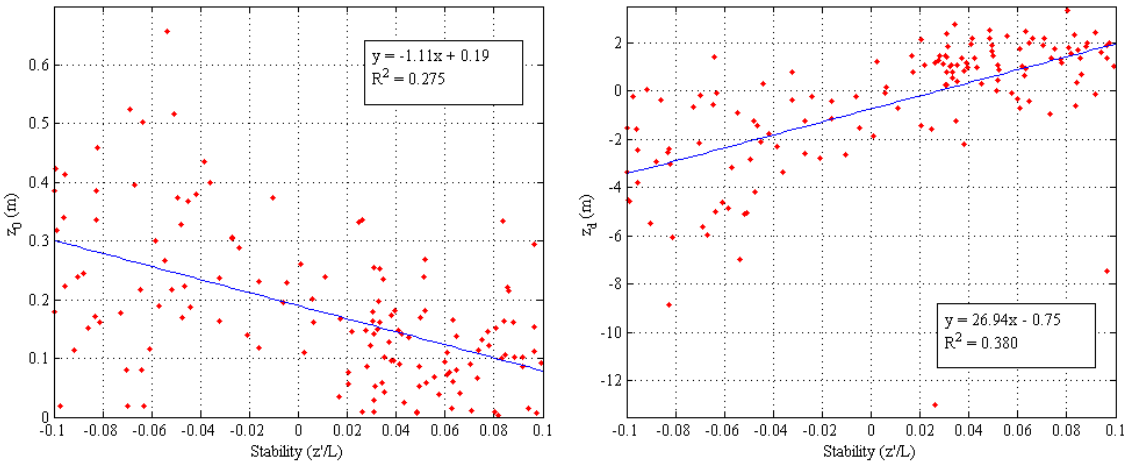

Figure 6: Estimated surface roughness length (z_0), left, and zero-plane displacement height (z_d), right, plotted as functions of the dimensionless stability parameter (z'/L) for all Sector V Event Week observation periods.

While the variability both within and between directional sectors is quite large, this scatter is common to anemometric methods of roughness parameter estimation (Al-Jiboori & Fei, 2005; Grimmond *et al.*, 1998; Rooney, 2001). The Ro method previously produced similar scatter around the estimated means and resulted in one sector with a

negative mean z_d (Rooney, 2001). Assuming a negative value can be interpreted as zero, the results for Sector V are in line with the expected behavior of z_d. Given the variability between the sectors and the large scatter in the estimates, it is important to note that the Ro method neglects the different sensor source area footprints that result from the difference in observation heights. The error caused by this could be substantial given the spatial heterogeneity of most urban areas and was a primary reason that fast-response observations from a single height were preferred to profile methods by Grimmond *et al.* (1998).

The scatter in anemometric estimates may be in part driven by variations in atmospheric stability despite the generally held assumption that z_0 and z_d are geometric parameters independent of the flow characteristics assuming neutral stratification. While all observations were filtered to include only near-neutral observation periods ($|\zeta| < 0$), plots of estimated z_0 and z_d as functions of stability both show distinctive trends even within this near-neutral range (Figure 6). In the case of z_0, the relationship is negative and slightly unstable periods ($-0.1 < \zeta < 0$) exhibit larger scatter than slightly stable periods ($0 < \zeta < 0.1$). For estimated of z_d, there is a positive relationship and a similarly large scatter for slightly unstable periods.

Based on the relationship shown in Figure 6, it appears that slightly unstable periods produce higher estimated z_0 than slightly stable conditions. This hypothesis matches the findings of Zilitinkevich *et al.* (2008) which showed a similar relationship extending beyond the range of near-neutral stratification. Additionally, there is greater scatter

between unstable observation periods as compared to stable ones. In the case of the Ro method, these slightly unstable periods are largely responsible for the unrealistic negative z_d estimates and the reason why mean z_d is much smaller than the median in Sector V during Event Week (Table 3).

5.2 Morphometric

The morphometric equations were applied using a series of input neighborhood sizes in order to determine the effect on the resulting surface parameters (Figure 7). Both z_d and λ_p show a peak at 100 m cell size. Below this size, the neighborhoods begin to approach the size of the roughness obstacles and above it, the neighborhoods tend to blend out roughness objects by including more and more area outside of the city. Overall, the effect of grid cell size results in just 10 cm maximum difference in resulting z_d. λ_f has a slight negative relationship with grid cell size, however the difference between the three smallest sizes (25, 50, and 100 m) is negligible and the resulting maximum difference in z_0 values is less than 2 cm. While these results do not provide an objective method for selecting a best grid cell size, they are encouraging because of the consistency of the results across this range. For the remainder of this section, results are reported using the 100 m neighborhood grid cells. While slightly below the recommended range in the literature, this area more closely represents the neighborhood scale in BRC.

The 100 m grid and the output surface parameters from the August 29th obstacle database are shown in Figure 8. Both λ_p and λ_f fall to 0 at the edge of the city and whereas λ_p seems to increase closer to the center, λ_f appears to vary more randomly throughout BRC. z_d follows a similar pattern to λ_p, increasing towards the city center although there are small pockets and corridors with low values. z_0 shows much more variation throughout the city and unlike z_d these values tend to spike on the outskirts of the city. Similarly, cells with high z_d tend to exhibit lower z_0, highlighting the relationship

between these two variables. Output z_0 and z_d for each individual grid cell is plotted in Figure 9. As expected, the Ma model follows the general heuristic arguments of Grimmond & Oke (1999): z_d approaches z_H as λ_p increases whereas z_0 peaks at an intermediate value of λ_p and then declines. From Figures 8-9 it can be seen that the frictional drag of surface varies throughout BRC due to changes in density and obstacle size.

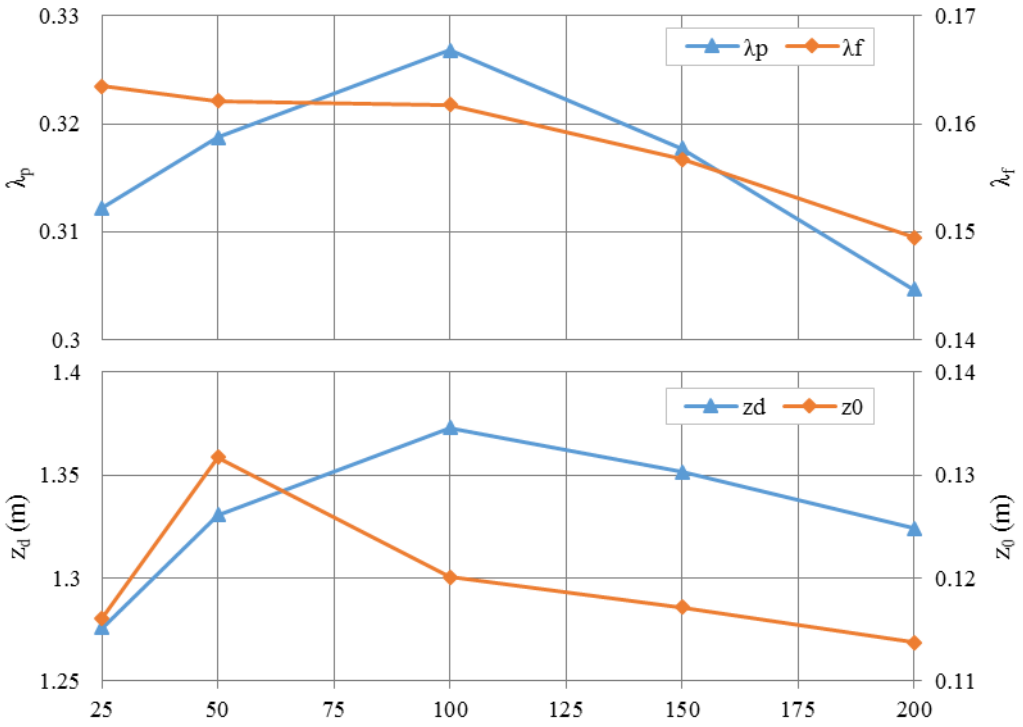

Figure 7: Effect of grid cell size on surface parameters for Black Rock City on August 29, 2013, Sector V.

Figure 10 shows the temporal trends in z_0 and z_d based on the down-sampled obstacle database and weighted based on the source area model using the mean conditions for all near-neutral observation periods. While these values are not directly based on observed

surface conditions, the rate of change in the number of surface obstacles is proportional to the estimated population of BRC on each day. The predicted trends show z_d increasing throughout this period with a spike on DOY 238 after the gates officially opened and then slowing as the population leveled out throughout the week. z_0 increases rapidly in the first 3 days before leveling out and actually decreasing slightly throughout the event for all directional sectors. When structures were absent or sparse, the addition of new obstacles created a rougher surface. As the city was filled in, the addition of new obstacles served to raise the mean momentum sink rather than increase the overall roughness. By DOY 238, the density of the city resulted in a skimming flow and the effective roughness of the city began to decrease.

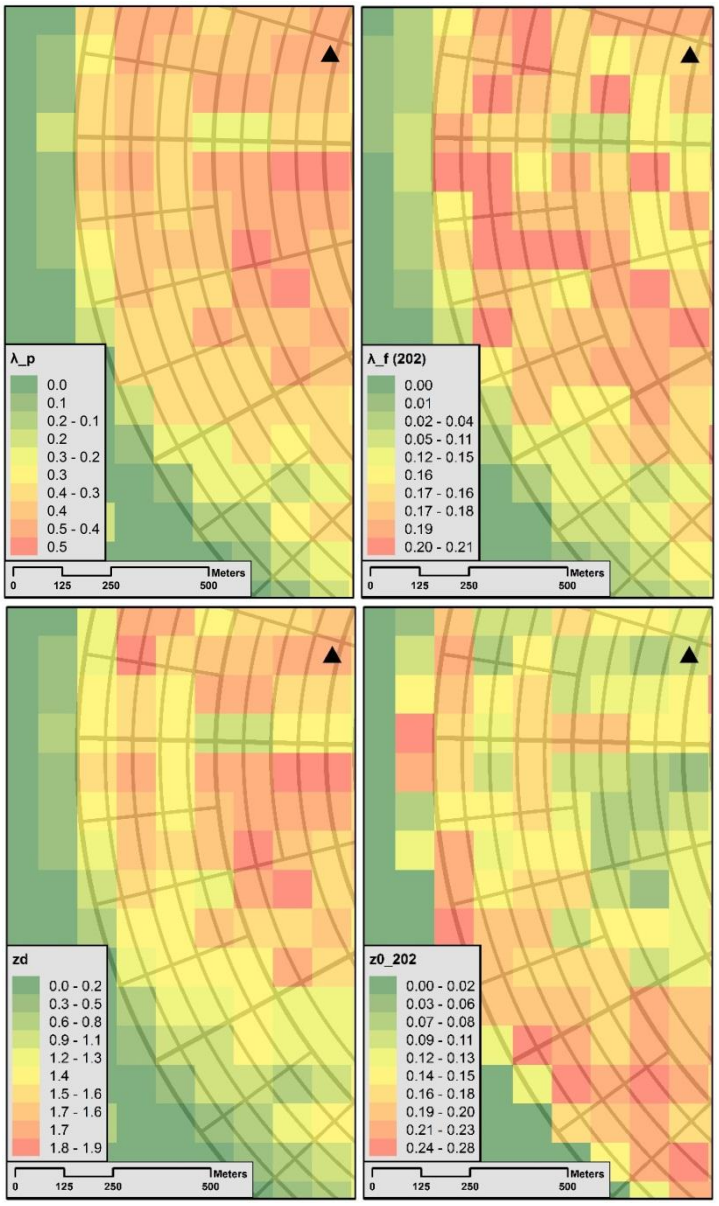

Figure 8: Plan area index, λ_p, (top-left), frontal area index, λ_f, (top-right), displacement height, z_d (m), (bottom-left), and surface roughness length, z_0 (m), (bottom-right) by 100 m grid cell for August 29, 2013 Black Rock City with street network.

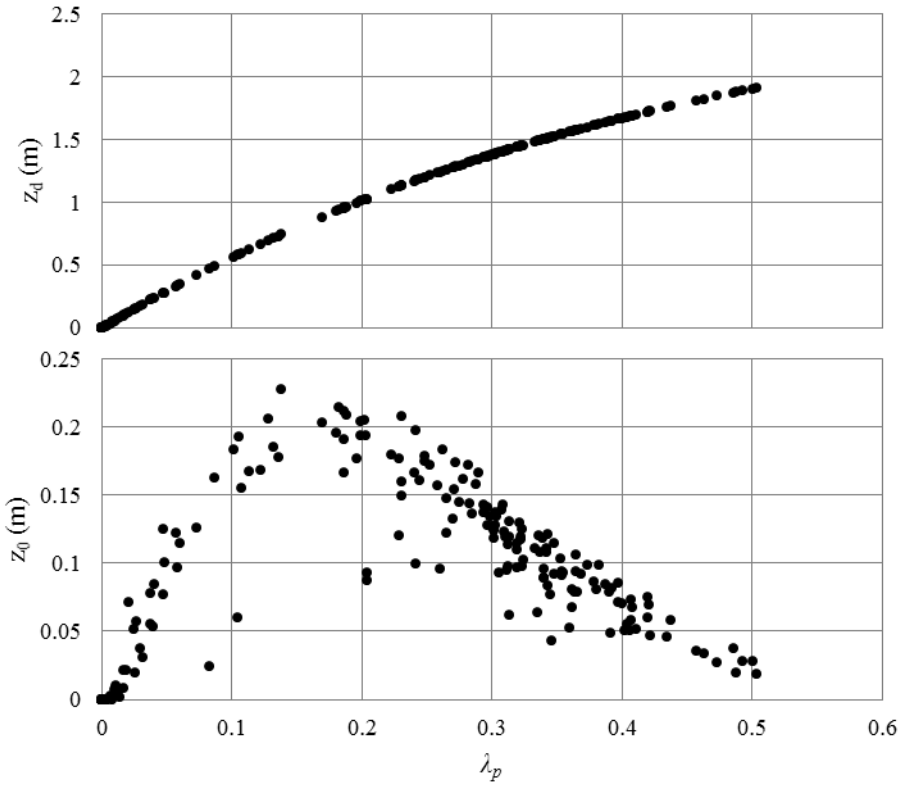

Figure 9: Morphometric output for 100 m grid cells showing the role of plan area index (λ_p) on zero-plane displacement height (z_d) and surface roughness length (z_0).

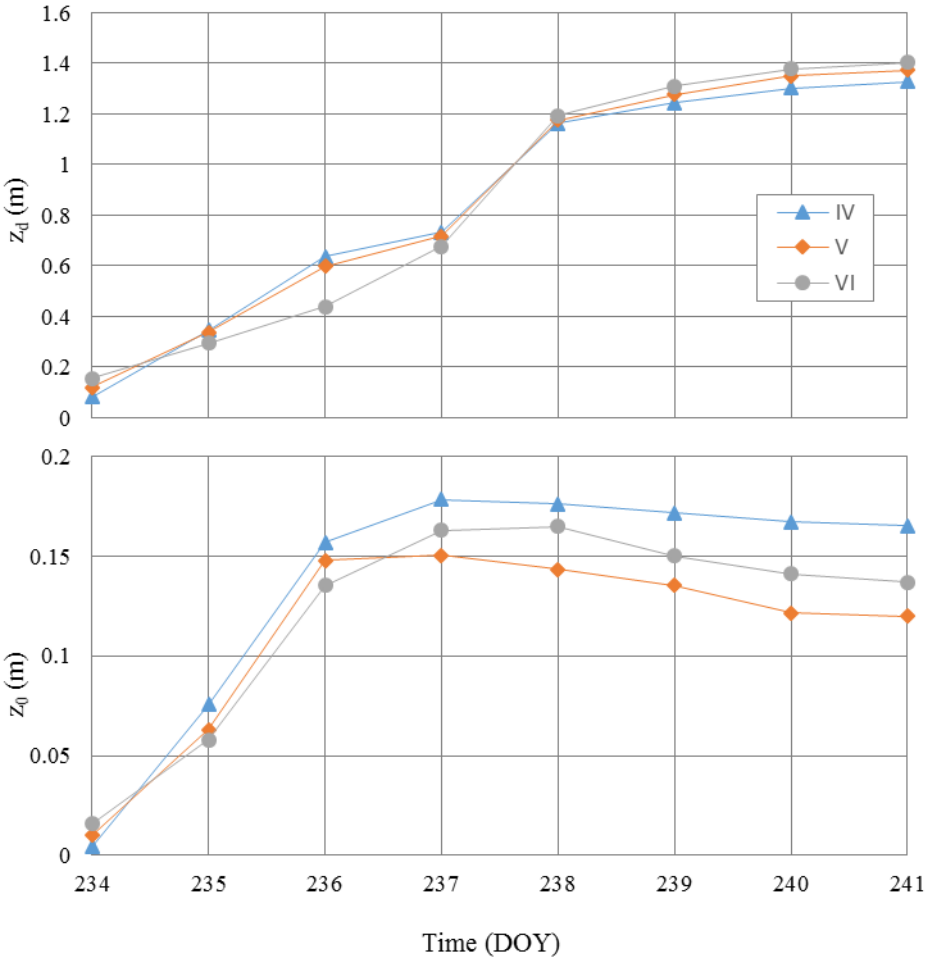

Figure 10: Time series of morphometric estimates of zero-plane displacement height (z_d) and surface roughness length (z_0) for Black Rock City for selected wind sectors.

5.3 Comparison

According to Grimmond & Oke, 1999, convergence between observed and modelled roughness estimates is not an assurance of either approach, however, these comparisons are the only method available to assess the reasonableness of each result. Despite this rather grim state-of-the-art, the anemometric and morphometric methods adopted here show general agreement. To provide further comparison, data for Sector V was again sub-divided for the Event Week Period in Table 5. Additionally, modified estimates and statistics for z_0 and z_d are provided using only slightly-stable conditions ($0 < \zeta < 0.1$) based on the large scatter and unrealistic estimates noted above.

Table 5: Estimated Statistics for Sector V Using Anemometric Methods

		Near-Neutral ($-0.1 < \zeta < 0.1$)		Slightly-Stable ($0 < \zeta < 0.1$)	
		z_0 (m)	z_d (m)	z_0 (m)	z_d (m)
Pre-Event: DOY 234-237	N	53	53	28	28
	Median	0.12	-1.23	0.07	0.32
	Mean	0.15	-1.76	0.10	-0.42
	SD	0.13	2.02	0.08	1.03
Event Week Part 1: DOY 238-241	N	25	25	16	16
	Median	0.17	0.69	0.14	1.73
	Mean	0.21	0.20	0.14	1.42
	SD	0.13	2.02	0.08	1.03
Event Week Part 2: DOY 242-246	N	63	63	44	44
	Median	0.15	1.07	0.14	1.33
	Mean	0.19	0.34	0.13	1.29
	SD	0.14	2.03	0.07	0.79

While the Ro method for z_d estimation resulted in negative estimates and large scatter, in general, this method showed that the momentum sink tended to increase between the Pre-Event and Event Week periods (Table 3). This is mirrored by the Ma method, which shows a consistent increase in z_d based on modeled surface cover (Figure 10). In its original form (including all near-neutral periods), the Ro method produces values that are below the modelled values from the Ma method (Table 5; Figure 6). This could be due to an overestimation of z_H or because the high porosity of many of the roughness obstacles is not captured by the Ma equations which were developed for bluff body obstacles (MacDonald *et al*., 1998). Alternatively, the higher values from the morphometric method may suggest that the median values from the Ro method are more representative than the means as these values both approach the Ma estimates and agree with the general rule-of-thumb that z_d is between one-half to two-thirds of z_H. When the slightly-unstable periods are removed, the scatter in estimated z_d falls substantially, the means are closer to the medians, Pre-Event estimated z_d is closer to zero, and the Event Period estimates are closer to the value modelled using the Ma method (Table 5). In this instance, the Ro method is greatly improved by the removal of these periods.

Based on the Es method, z_0 appears to increase slightly between the Pre-Event and Event Week periods matching the trend of the Ma method (Table 4; Figure 10). In the observational data, mean z_0 was initially greater than expected during the Pre-Event period, however, this value falls when removing the slightly stable periods (Table 5). While the Es method failed to reproduce the same rapid increase shown by the Ma

method, it is likely there are insufficient Pre-Event observations to capture the much lower z_0 values modeled on DOY 234-235. As seen in Figure 2, there were existing roughness elements in the predominant wind direction at the start of the experiment and their number increased steadily leading up to the event's official start. The change in mean z_0 between Pre-Event and Event Week was smaller than expected as a result of this early development, however the Ma method predicts that z_0 was actually very small (~1 cm) on DOY 234 (Figure 10). Furthermore, modelled z_0 peaked between DOY 236 and 237, the final day of the Pre-Event observation window.

Another reason for the small change in z_0 between the Pre-Event and Event Week periods is the development of $z_d > 0$. These results are similar to those of Rooney (2001), who found that increased building density in the upwind area resulted in increased z_d and decreased z_0. A comparison of Sectors V and VI anemometric estimates shows a similar pattern: in Sector VI where z_d is assumed to be zero based on the negative estimated mean z_d, the mean z_0 is higher than Sector V where $z_d > 0$. However, this trend is not corroborated by the morphometric estimates (Tables 3-4).

Compared to the observational methods, the morphometric technique did not capture any major directional differences in estimated z_0 or z_d (Tables 3-4; Figure 9). This may be due to the fact that z_H was not allowed to vary and that the differences seen by the Es and Ro methods across sectors may be largely a product of height variability rather than the area indices. Similarly, the Ma method appears to underestimate z_0 as compared with the observational estimates, especially for Sector VI (Table 4; Figure 10). This may be due to

the selected value for z_H or may be a product of the selected model. Grimmond & Oke (1999) note that Ma results in values of z_0 that are too small when $\lambda_p > 0.4$. Additionally, more recent studies have shown that surfaces with a high standard deviation of obstacle heights, a factor not considered in this analysis, result in higher effective z_0 values (Millward-Hopkins *et al*., 2011b).

Table 6: Comparison of Surface Parameters for Urban Areas

Location	Description	*Ma:* z_d	*Ma:* z_0	*Es:* z_0	z_H	λ_p	λ_f	z_d/z_H	z_0/z_H
Black Rock City, NV*	*medium density*	1.37	0.12	0.20 ±0.13	2.5	0.33	0.16	0.55	0.08
Sapporo, Japan**	*low density* - single 2-story houses, gardens, some trees	*Na*	*Na*	0.30	7.0	0.25	0.19	Na	0.12
Miami, FL**	*low density* - single 1- or 2-story houses, gardens, and trees	*Na*	*Na*	0.46 ±0.60	6.9	0.41	0.18	Na	0.07
Worcester, MA**	*medium density* - mixed houses, large trees	*Na*	*Na*	0.91 ±0.27	13	0.38	0.12	Na	0.07
St. Louis, MO**	*medium density* - closely space 2-story hours, large trees	*Na*	*Na*	1.09	9.7	0.5	0.12	Na	0.11
Los Angeles, CA***	Downtown	23.8	6.00	*Na*	44	0.29	0.38	0.54	0.14
Los Angeles, CA***	Residential	5.70	0.74	*Na*	10	0.27	0.12	0.57	0.07
Los Angeles, CA***	Industrial	4.70	0.15	*Na*	7	0.38	0.1	0.67	0.02

* Estimated values for Sector V. Ma taken from DOY 241 and Es from mean of Event week observations.
** Source: Grimmond & Oke (1999)
*** Source: Di Sabatino *et al*. (2010)

The results of this analysis are compared with other urban areas in Table 6. As noted earlier, the scatter in anemometric estimates is similar to previous studies. Estimated z_0 for Sectors V is lower than that commonly found above suburban areas which range

between 0.4 - 0.7 m and much lower than dense urban areas where this value generally exceeds 1.0 m (Tables 1 and 6). In addition to the structure heights being lower than a typical suburban area, the porosity of the roughness elements in BRC likely served to lower z_0 as well, resulting in z_0 closer to the industrial zone from Los Angeles, CA listed in Table 6 or grain crops listed in Table 1. Based on the non-dimensional ratios in Table 6, BRC ranks within the "Medium density – wake interference flow" category from Grimmond and Oke (1999) study (See Table 7 from referenced paper). This puts BRC in the same category as the Worester, MA and St. Louis, MO sites despite the lower estimated z_0.

5 Conclusion

This paper presents anemometric and morphometric estimates of z_0 and z_d modifications in BRC. The construction of a large, densely populated city caused a measurable impact on the surface layer wind profile. Estimated z_0 values were much larger than a typical playa surface but remained smaller than a typical urban or suburban area possibly as a result of both the lower structure height and higher porosity relative to a typical North American city. According to the Ma model, z_0 increases sharply just prior the start of the event and remains nearly constant throughout the event. In contrast, z_d increases steadily throughout the study period showing how after object density reaches a threshold ($\lambda_p \approx 0.2$), increasing the number of obstacles raises the momentum rink rather than increases overall roughness. Within the predominant wind direction (Sector V), the observational methods show an increase in z_0 following the pre-Event period and no change within the event period and z_d shows a large increase between the pre-Event and Event periods. While sparse, the anemometric estimates corroborate the general trends of the Ma method.

Similar to previous studies that rely on observational methods, the scatter in the resulting estimates was large relative to the estimated magnitudes. Shorter averaging periods may help increase the sample size and allow for more refined directional and temporal estimates. Despite limiting the analysis to periods of near-neutral stability, there is still a relationship between the atmospheric stratification and estimated roughness values which may be a source of the scatter seen here and in other observational

campaigns. Despite the scatter, the Es method appears to perform well despite being ill suited to short observation campaigns where the surface cover is rapidly changing. The Ro method resulted in much higher scatter and unreasonable estimates in many cases, raising questions about the validity of this method. With the removal of all slightly-unstable periods, the scatter in the Ro and Es estimates decreased and produced more theoretically reasonable results.

Based on the modeled surface inputs, the Ma method correctly predicted the change in the surface roughness parameters as compared to the observational estimates. Based on these results, the model appears valid for use in BRC or other temporary cities in combination with average height estimates and satellite imagery. While useful in attempting to validate the anemometric values, the Ma model did not capture the same directional variation. This may be a result of the model limitations at high densities or because of the single assigned z_H used in this study. Future work of this type could attempt to include a more detailed obstacle classification to estimate average obstacle height or use structure-from-motion or shadow-length to calculate individual objects heights directly.

6 Bibliography

Afterburn.burningman.com,. (2014). Burning Man :: AfterBurn Report 2013. Retrieved 13 August 2014, from http://afterburn.burningman.com/13/

Al-Jiboori, M. H., & Fei, H. U. 2005. Surface roughness around a 325-m meteorological tower and its effect on urban turbulence. *Advances in Atmospheric Sciences*, *22*(4), 595-605.

Comparison: Peak Populations in 2012 and 2013. (2014). Black Rock City Census. Retrieved from http://blackrockcitycensus.wordpress.com/2014/07/01/comparison-peak-populations-in-2012-and-2013/

Bottema, M, 1997. Urban Roughness Modelling in Relation to Pollutant Dispersion. *Atmospheric Environment*, Vol. 31, No. 18, pp 3059-3075.

Clements, C. and Oliphant, A.J., 2014. The California State University- Mobile Atmospheric Profiling System (CSU-MAPS): A facility for research and education in boundary-layer meteorology. *Bulletin of the American Meteorological Society* (in press).

Di Sabatino, S., Leo, L., Cataldo, R. 2010. Construction of Digital Elevation Models for a Southern European City and a Comparative Morphological Analysis with Respect to Northern European and North American Cities. *Journal of Applied Meteorology*, *49*, 1377-1396.

Grimmond, C. S. B., King, T. S., Roth, M., & Oke T. R. 1998. Aerodynamic roughness of urban areas derived from wind observations. *Boundary-Layer Meteorology*, *89*(1), 1-24.

Grimmond, C. S. B., & Oke, T. R. 1999. Aerodynamic properties of urban areas derived from analysis of surface form. *Journal of Applied Meteorology*, *38*(9), 1262-1292.

Grimmond, C. S. B., & Souch, C. 1994. Surface Description for Urban Climate Studies: A GIS Based Methodology. *Geocarto International, (1) 1994*, 47-59.

Hsieh, C., Katul, G., Chi, T. 2000. An Approximate Analytical Model for Footprint Estimation of Scalar Fluxes in Thermally Stratified Atmospheric Flows. *Advances in Water Resources*, 23 (2000): 765-772.

Holland, D. E., Berglund, J. A., Spruce, J. P., & McKellip, R. D. 2008. Derivation of effective aerodynamic surface roughness in urban areas from airborne lidar terrain data. Journal of Applied Meteorology and Climatology, 47(10), 2614-2626.

Joy, S.L. 2011. Evaluation of Analytical Footprint Models and Energy Balance Closure Methods Over Cotton in Texas Panhandle (Master's Thesis, Colorado State University).

Liu, G., Sun, J., & Jiang, W. 2009. Observational verification of urban surface roughness parameters derived from morphological models. *Meteorological Applications*, *16*(2), 205-213.

MacDonald, R. W., R. F. Griffiths, and D. J. Hall, 1998: An improved method for estimation of surface roughness of obstacle arrays. *Atmos. Environ.*, **32,** 1857–1864.

Millward-Hopkins, J.T., Tomlin, A.S., Ma, L., Ingham, D.B., Pourkashanian, M. (2011a). Aerodynamic Parameters of a UK City Derived from Morphological Data. *Boundary-layer meteorology*, *146*(3), 447-468

Millward-Hopkins, J. T., Tomlin, A. S., Ma, L., Ingham, D., & Pourkashanian, M. (2011b). Estimating aerodynamic parameters of urban-like surfaces with heterogeneous building heights. *Boundary-layer meteorology*, *141*(3), 443-465.

Oke, T. R. 1988. *Boundary layer climates*. Routledge.

Oke, T 2006. Initial Guidance to Obtain Representative Meteorological Observations at Urban Sites. *World Meteorological Organization, Instruments and Observing Methods, Report No. 81.*

Powell, M., Soukup, G., Cocke, S., Gulati, S., Morisseau-Leroy, N., Hamid, S., Dorst, N, and Axe, L. 2005. State of Florida hurricane loss projection model: Atmospheric science component. *Journal of wind engineering and industrial aerodynamics*, 93(8), 651-674.

Rooney, G. G. 2001. Comparison of upwind land use and roughness length measured in the urban boundary layer. *Boundary-layer meteorology*, *100*(3), 469-485.

Wieringa, J., Davenport, A., Grimmond, C.S.B., Oke, T. 2001. New Revision of Davenport Roughness Classification. *Proc., 3rd European & African Conf. on Wind Engineering, Eindhoven, The Netherlands*, 285-292.

Wieringa, 1993. "Representative Roughness Parameters for Homogeneous Terrain." *Boundary Layer Meteorology*, Vol. 63, Issue 4, pp. 323-393.

van Wijk, B.M., 2011. Predicting the Rooftop Wind Climate for Urban Wind Energy in the Rotterdam-Delft-Zoetermeer Region: New Approaches for Implementing Urban Height Data in the Wind Atlas Method (Master's Thesis, Eindhoven University of Technology).

Zilitinkevich, S. S., Mammarella, I., Baklanov, A.A., Joffre, S.M., 2008. The Effect of Stratification on the Aerodynamic Roughness Length and Displacement Height. Boundary-Layer Meteorology 129:179-190.